Experimental Study on the Relationship between Direction of Crack Propagation and Thermal Stress Distribution in Laser Cleaving Process for Glass Substrate

Yuki Nakajima*, Keiji Yamada*, Kazuki Fukushima**, Ryutaro Tanaka* and Katsuhiko Sekiya*

*Graduated School of Engineering, Hiroshima University, 1-4-1 Kagamiyama, Higashi-Hiroshima 739-8527, Japan
E-mail: keiji@hiroshima-u.ac.jp
** Sodick Co., Ltd. 3-12-1, Nakamachidai, Tsuzuki-ku, Yokohama, Kanagawa, 224-8522 Japan

Photoelastic observation was applied for the thermal stress cleaving of brittle substrates in order to experimentally investigate the stress distribution and its effects on the accuracy of crack propagation. In the laser cleaving process with a curved path, the principle stress acted on the incorrect direction near the edge of the substrate, then the crack deviated from the desired cleaving path. Additionally, high scanning speed of laser disturbed the distribution of the principal stress direction and resulted in the incline of cleaved surface. In the trimming process by laser cleaving, the straight cleaving path was bent toward the free edge of substrate due to the asymmetrical stress distribution, which was successfully observed by the proposed photoelastic method.
DOI: 10.2961/jlmn.2019.02.0008
Keywords: laser cleaving, brittle substrate, trimming, thermal stress, photoelastic observation

1. Introduction

A large variety of information devices need brittle material substrates such as glass panels for display, dies of CPUs and memory chips and so on. These substrates are mechanically cut off from the large size ones on which the electrical and optical functions are already constructed. Diamond sawing and scribing are conventionally used for this process [1], but the major concerns are undesired fracture of substrates and the low productivity.

Laser cleaving is yet another process to cut or dice a variety of brittle substrates not by mechanical tools but by thermal crack propagation [2-6]. Laser irradiation yields temperature distribution in the vicinity of laser spot, which causes compression within the spot and circumferential tension around the spot. The crack in tensional field propagates toward the center of spot, if tensile stress is enough high. Therefore, moving the laser spot at appropriate speed, the crack follows it and then the substrate is divided along the laser scanning path. This process has advantages such as high speed and high flexibility of the path, and high yield rate due to the small kerf loss. In addition, the substrates are free from the contamination by chips and are immune from the fracture by machining force.

However, accuracy of the process often can be a problem under asymmetrical distribution of temperature and/or stress. For example, the crack deviates from the laser scanning path when the path is close to the edge of substrates [7] and the curved path is employed [8]. This is because the crack propagation is controlled by stress distribution, not by any other means including tools and dies.

In order to elucidate mechanism of the process and to investigate influences of the process parameters on the accuracy of crack propagation path, the distribution of temperature and stress has been theoretically analyzed by many researchers [4, 8, 9]. For example, Tsai et al. proposed to repeat trial cuts by varying the parameters to decrease the deviation of crack propagation path and improve the process accuracy [10]. These approaches all are effective methods for the research in laboratories, but cannot be used for the in-process inspection on manufacturing sites.

Therefore, authors proposed a photoelastic technique to visualize the distribution of thermal stress within the substrate during the laser cleaving process. In the previous paper, feasibility of the proposed method was examined and the asymmetrical stress distributions were presented under several conditions of laser cleaving process [11]. In this study, the photoelastic method is used to observe and investigate stress distribution in the laser cleaving process of substrates. Trimming by laser cleaving and curvilinear path cleaving are conducted to demonstrate the feasibility of the proposed detecting method for the asymmetry which degrades the process accuracy.

2. Experimental procedure

Cleaving tests were conducted to investigate the stress distributions and their influence on the process performance. The heat source for the process was a CO_2 laser (Coherent Diamond C-20, wave length = 10.6 μm), which was obliquely irradiated on the crown glass substrate (dimension: 76×26×1.2 mm) in which initial defect was previously introduced. The experimental set-up was built on the table of a CNC machine tool, while the substrate was mounted on a spindle head of the machine tool in order to move the laser spot in the arbitrary path on substrate and with the controlled speed. Two kinds of laser scanning paths used were as follows.

2.1 Curvilinear cleaving process

Table 1 shows the conditions for cleaving test with a curvilinear scanning path shown in **Fig. 1**. The path started from the initial defect introduced at the long side edge of a substrate, and formed an arc with a radius of 21.9 mm, and finally ended at the other point on the same edge. The initial defect was a 1 mm length crack introduced by a diamond scriber. The laser spot moved at a scanning speed V (= 50, 80, 100, 130 mm/min) on this circular arc path. Consequently, the material surrounded by the circular arc path and the edge of substrate was cut out when the crack continuously propagated without stagnation.

The curved paths cause temperature distribution asymmetrical with respect to the path. This effect was investigated by photoelastic observation. And, the crack propagation direction was discussed by means of the distribution of principal stress direction in the vicinity of crack tip, which was derived from isoclinic fringe patterns.

Table 1 Conditions in curvilinear cleaving tests

Laser pulse frequency	f (kHz)	20
Duty factor	(%)	10
Average laser power	Q (W)	4.2
Size of laser spot	(mm	3 × 2

Table 2 Conditions in trimming tests

Laser pulse frequency	---	CW
Average laser power	Q (W)	6.0
Size of laser spot	(mm)	φ 4.0

Table 3 Properties of glass substrates

Refractive index		1.524
Young's modulus	(GPa)	71
Poisson ratio		0.224
Density	(kg/m^3)	2590
Thermal conductivity	(W/m K)	0.95
Specific heat	(J/ kg K)	783
Coefficient of linear expansion	(1/K)	9.6×10^{-6}

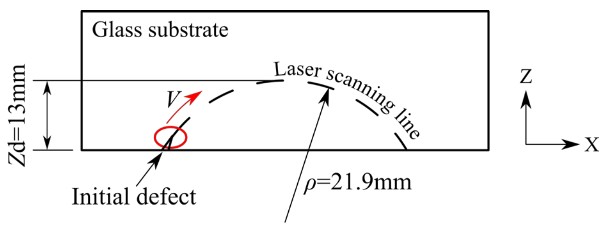

Zd: Vertex height of arc from substrate edge
ρ: Curvature radius of laser scanning path
V: Scanning speed (= 50, 80, 100, 130 mm/min)

Fig. 1 Curvilinear cleaving experiment.

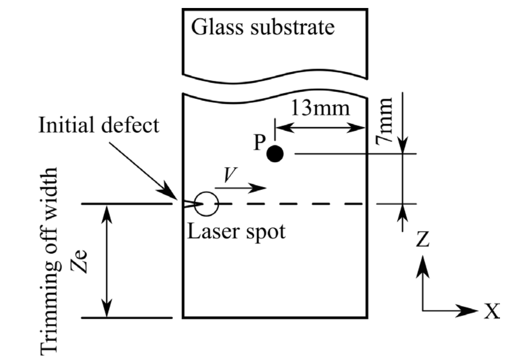

Fig. 2 Trimming experiment by laser cleaving.

2.2 Trimming process

Figure 2 shows a methodology in trimming test which was conducted under the conditions shown in Table 2. The straight laser scanning path was parallel to the short side edge of substrate with a distance of *Ze*, which corresponded to a width of the portion of substrate trimmed off.

The trimming path also could cause asymmetrical distribution of temperature, so that this effect was investigated by photoelastic observation. And, the asymmetry of observed fringe patterns was quantified and evaluated by image data processing. In addition, the principal stresses difference distribution was drawn to illustrate the distribution of shear stress in the vicinity of crack tip, which are said to cause the deviation of crack path [9].

All experiments were conducted for the glass substrates whose properties are shown in Table3, in this study [12].

3. Principle and method for stress analysis

Figure 3 shows a linear polariscope for isoclinic observation used in the laser cleaving experiments to obtain the fringe pattern [11]. It consists of a light source S, a transparent substrate W, a camera O, and a pair of polarizers $P_1$and P_2 whose optic axes are perpendicular to each other. It should be noted that a pair of quarter-wave plates and a bandpass filter (@546nm) are also needed for a circular polariscope to obtain isochromatic fringe pattern.

When a ray of light passes a photoelastic material, intensity of the light I emerging from the polarizer P_2 is given by

$$I = A^2 \sin^2 2\varphi \sin^2 \frac{\delta}{2} \tag{1}$$

where A is an amplitude of the light transmitted, and φ is an angle indicating the principal stress direction from the optic axis of polarizer. And δ is a relative retardation that is given by the stress-optic law as

$$\delta = 2\pi d(\sigma_1 - \sigma_2)C/\lambda \tag{2}$$

where d is the material thickness, C is a stress optic coefficient of the material, λ is a wavelength of light, and σ_1 and σ_2 are principal stresses [13]. Eq. (1) indicates that the light becomes extinct (I=0) with $\sin^2 2\varphi = 0$ or $\sin^2(\delta/2) = 0$.

3.1 Distribution of principal stress direction

Isoclinic and isochromatic lines are both observed in the fringe pattern obtained by the linear polariscope as shown in eq. (1). But, using white light as the source, the relative retardation δ can be neglected and the isoclinic fringe pattern can be obtained. **Figure 4** shows the isoclinic pattern captured for the optic axis of polarizer θ= 0°, and the isoclinic lines extracted from the pattern, which are the loci of the points where the principal stress coincides with the orientation of polarizer (= $\{(x, z) \mid_{\varphi = 0 \text{ or } \pi/2}\}$, $\theta = 0°$). Rotating the polarizers to obtain the isoclinic lines for different optic axes θ, we can find the distribution of principal stress direction within the material.

3.2 Distribution of principal stress difference

An isochromatic fringe pattern is captured by means of the circular polariscope that includes a pair of quarter-wave plates and a bandpass filter. Isochromatic lines in the pattern are the loci of the points where the difference of principal stresses (σ_1 - σ_2) remains particular value which corresponds to $\delta = 2n\pi$ ($n = 0, 1, 2\ldots$). Therefore, distribution of principal stress difference can be obtained from the observed pattern.

However, it is difficult to identify the value of the principal stresses difference (σ_1 - σ_2) for the materials such as glasses whose optic coefficient C is small. Therefore, in this study, 2 orthogonal strains ε_x and ε_z are measured with strain gauges during the laser cleaving tests, and the principal stresses difference was obtained as follows.

In the cleaving tests, the strain gauges were attached enough away from the laser scanning path in order to evade the influence of the high temperature. At this measuring point, stresses σ_x, σ_z and τ_{zx} are calculated by following equations with a Poisson ratio ν.

$$\sigma_x = \frac{E(\varepsilon_x + \nu\varepsilon_z)}{1-\nu^2}, \sigma_z = \frac{E(\varepsilon_z + \nu\varepsilon_x)}{1-\nu^2} \quad (3)$$

$$\tau_{zx} = \frac{\sigma_x - \sigma_z}{2}\tan(\varphi - \theta) \quad (4)$$

where (φ-θ) is an angle indicating the principle stress direction from x-axis as shown in Fig. 1. This angle was derived from the distribution of principal stress direction mentioned in previous section.

Next, the following relation was used to convert the measured stresses to the principal stresses difference (σ_1 - σ_2) and at the measuring point.

$$\tau_{\max} = \frac{\sqrt{(\sigma_z - \sigma_x)^2 + 4\tau_{zx}{}^2}}{2} = \frac{\sigma_1 - \sigma_2}{2} \quad (5)$$

In order to obtain the stress difference distribution in the vicinity of the laser scanning path, we previously obtained the correspondence of the principal stresses difference to the intensity in isochromatic fringe pattern. And finally, the stress difference distribution was derived with reference to the correspondence.

3.3 Plotting stress distributions

Figure 5 shows procedure to obtain the distribution of principal stress difference near the tip of crack propagating during the laser cleaving process. Strain gauges are attached at the center of the substrate P to measure the normal strains ε_x and ε_z when the laser spot reaches the center of substrate. It should be noted that the maximum temperature rise was not more than 40 °C at the point P in the laser cleaving process. Therefore, the influence on the measured strains was less than 0.1 % by referring to the spec sheet of strain gauges. Substituting the measured strain values to Eq. (3) yields normal stresses σ_x, σ_z.

Then, the principal stress direction (φ-θ) is obtained from an isoclinic fringe pattern captured when the laser spot reaches the center of substrate. The shear stress τ_{zx} is obtained at point P in the isoclinic fringe pattern by substituting the direction to Eq. (4), while Eq. (5) yields the principal stress difference (σ_1 - σ_2) at the same point.

Finally, the distribution of brightness is converted to one of the principal stress difference (σ_1 - σ_2) at the optional po-

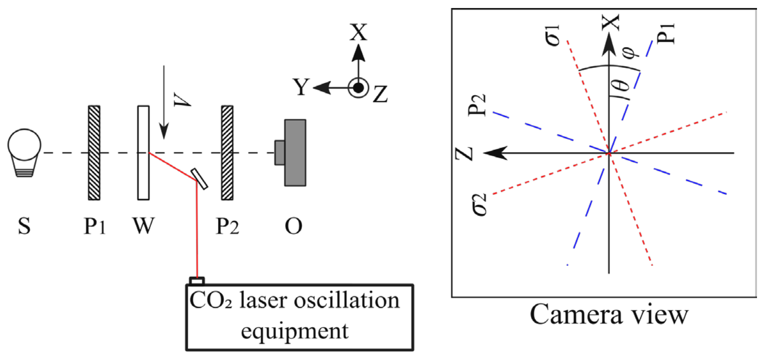

S : White light source O : Digital camera
P1, P2 : Polarizer V : Scanning speed
W : Glass substrate

Fig. 3 Experimental system for isoclinic fringe observation

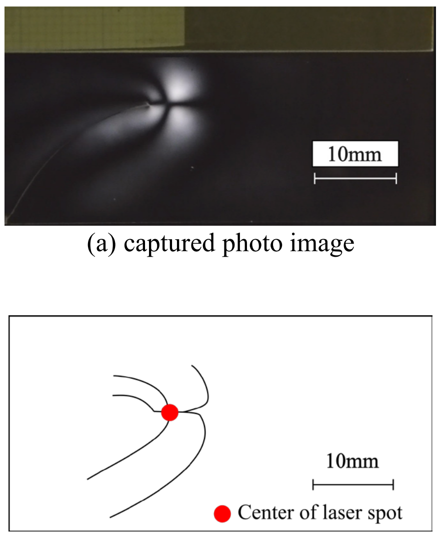

(a) captured photo image

(b) isoclinic lines

Fig. 4 Isoclinic lines extracted

sition within an isochromatic image by referring to the correspondence between the principal stress difference and the brightness at point P in isochromatic fringe pattern.

4. Experimental results and discussions

4.1 Results in curvilinear cleaving process

As mentioned above, the circumferential tension around the laser spot propagates the crack toward the spot center. Thus, the crack opening effect is dominant in the laser cleaving process [4], i.e. it is due to the mode I fracture (opening mode) in fracture mechanics [14]. Therefore, principal stress direction indicates the propagation direction of crack.

Figure 6 gives examples of fringe pattern and the distributions of principal stress direction near the crack tip in the laser cleaving test with a curved path under constant scanning speed: V= 100 mm/min. Figure 6(a) was obtained from the isoclinic fringe pattern, which was captured when the crack tip was propagating at the center of substrate. On the other hand, Fig. 6(b) was obtained from the isoclinic fringe pattern captured when the crack tip was propagating near the free edge of the substrate, which is represented by a red sloid line in the figure.

In both of Figs. 6(a) and 6(b), the curved solid lines show the direction of principal stress generated, and the long and short dashes lines represent the laser scanning paths along which the crack was intended to propagate. Besides, a dotted line represents an actual path of crack propagation in Fig. 6(b).

Fig. 6(a) shows that the principal stress direction is perpendicular to the laser scanning path in just front of the crack tip. This demonstrates that the thermal tensile stress opened the crack to propagate toward the laser spot. Thus, the deviation of crack is not found in this figure. However, in Fig. 6(b), the direction of principal stress is not perpendicular but inclined to the laser scanning path. Thus, the crack propagation path was bent inward, although the crack propagated

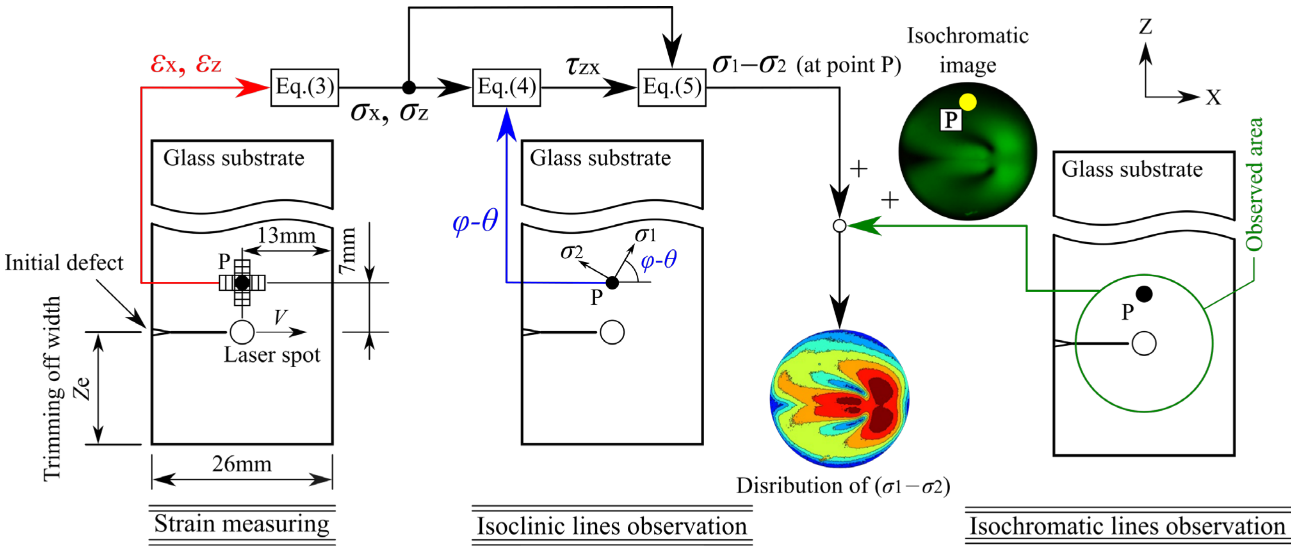

Fig. 5 Procedure to obtain distribution of principal stress difference (σ_1 - σ_2).

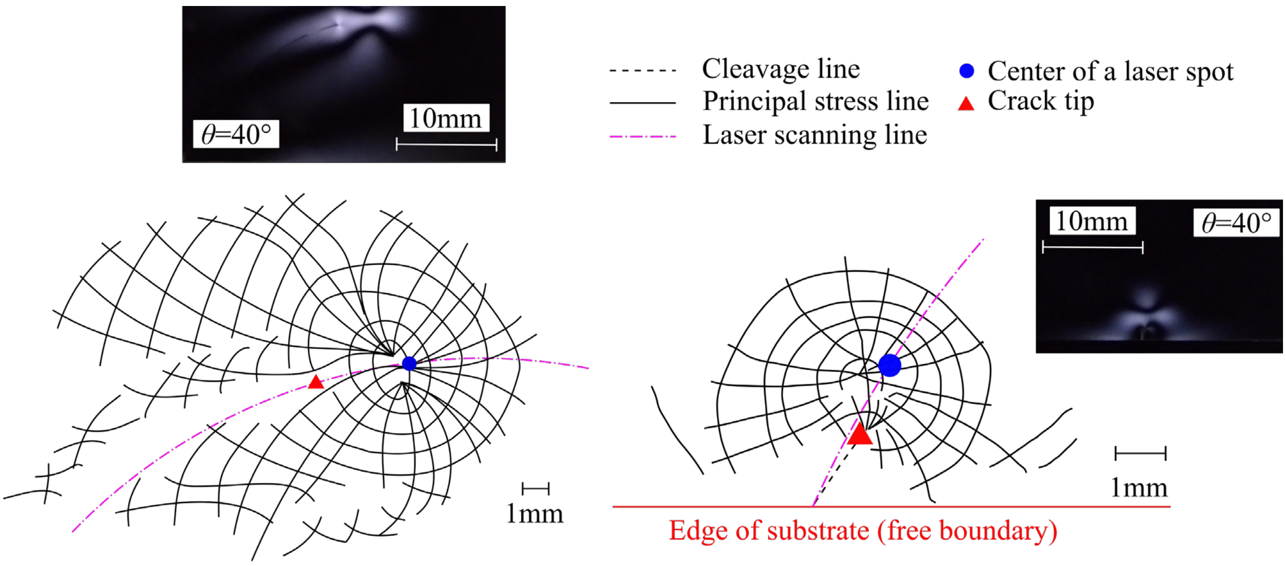

(a) at center of substrate (b) near edge of substrate

Fig. 6 Influence of crack tip position to distribution of principal stress direction (V = 100 mm/min).

from the initial defect on the edge as shown in this figure. This deviation was due to that the edge of substrate was a thermally insulated boundary and was also a mechanically unconstrained boundary which cause asymmetry on temperature and stress within the substrate.

The effect of boundary decreased when the crack tip reached the middle of curved path, and thus the crack deviation became small. But, the cleaved surface slightly twisted for high scanning speed. **Figure 7(a)** illustrates the twisted cleaved surface and a gap between upper and lower edges of the cleaved surface Δ. In Fig. 7(b), the photographs of gaps for the laser scanning speed V=50 and 100 mm/min are shown as examples. Green and blue curved lines represent the upper and the lower edge, respectively in these figures. Detailed microscopic observation revealed that the twist of cleaved surface and the gaps were caused by the outward deviation of lower edge under the conditions in this study.

Figure 8 gives a distribution of the gap Δ along the curvilinear scanning path for several scanning speeds. An optical microscope was used to measure the gaps at each point shown in Fig. 8(a). Three samples were used for each scanning speed for this measurement and the averaged values are shown in Fig. 8(b). The gap was not observed at the beginning and end of scanning (θ_m = 0, 180°), while the gap increased at the center of path. It also can be seen that the gap increased with the speed, but the distribution of gap was disturbed for V=80 mm/min. The cause of this would be investigated by further experiments.

Figure 9 shows two examples of the distributions, which were obtained from the isoclinic fringe pattern for the scanning speed of 50 and 100 mm/min. In these figures, positions of laser spot and crack tip are shown, and the distance between spot and crack tip is also indicated as d. The distance was large for the high speed but small for the low speed. For low speed of scanning V=50 mm/min, the distribution of principal stress direction formed concentric circles with the laser spot as shown in Fig. 9(a). Thus, the circumferential tensile stress provided high followability of crack to the laser spot motion and high accuracy of cleaving path. Besides, for high scanning speed, the distance d was large and the distribution of principal stress direction formed ellipses as shown in Fig. 9(b). The increased distance depressed an effect to propagate the crack toward the spot center especially on lower edge, thus the lower edge deviated outward. This would be because the gap Δ was yielded for high laser scanning speed.

The results in this section have shown that the distribution of principal stress direction provided important aspects for improving the laser cleaving process with curvilinear path.

4.2 Results in trimming process

The boundary effect is found as deviation of crack propagation in the trimming process by laser cleaving. **Figure 10** shows examples of isoclinic fringe obtained for the trimming width Ze of 15 and 5 mm, which both were captured when

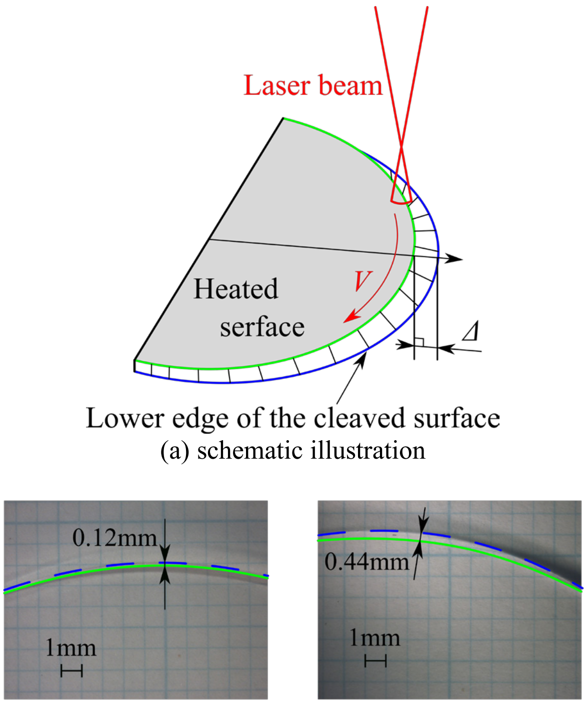

(a) schematic illustration

V=50 mm/min V=100 mm/min

(b) cleavage surface

Fig. 7 Distortion of cleavage surface.

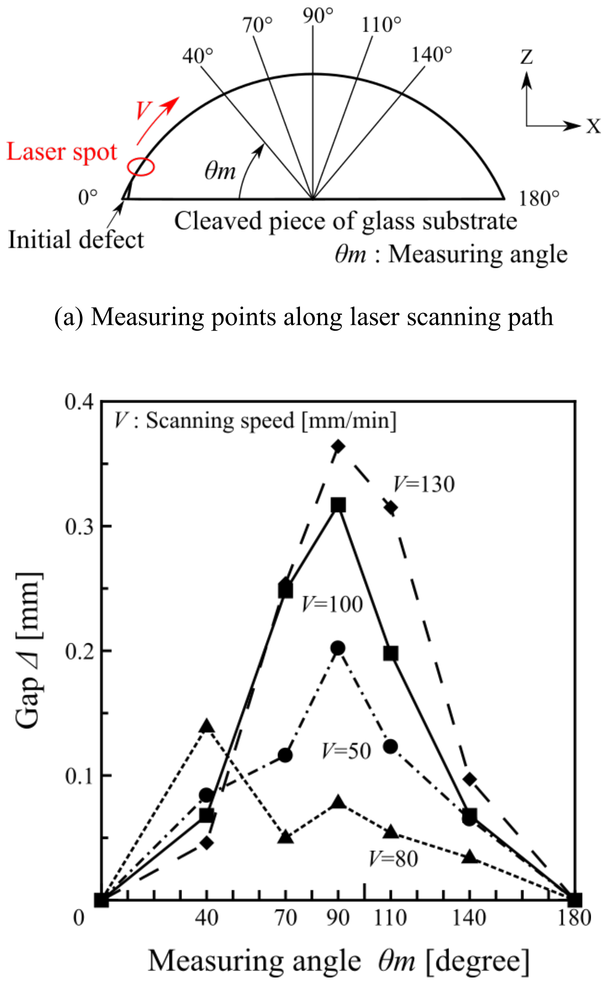

(a) Measuring points along laser scanning path

(b) Distribution of gap along laser scanning path

Fig. 8 Variation of gap Δ between upper and lower edge for different scanning speeds V.

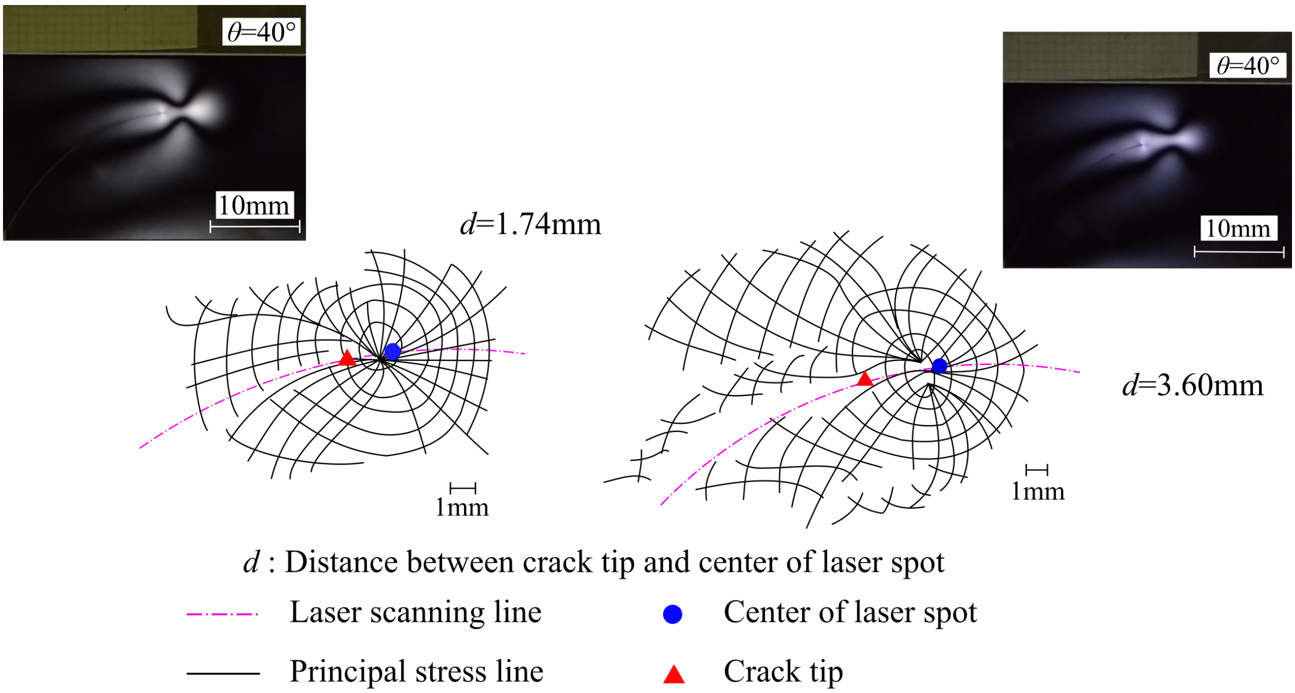

(a) V=50 mm/min (b) V=100 mm/min

Fig.9 Influence of scanning speed V to distribution of principal stress direction.

the laser spot reached the center of substrate. It is obvious from the figure that the fringe pattern was asymmetrical when the trimming width was small. Crack propagation path deviated from the laser scanning path for Ze =5 mm, while a straight cleaving was achieved for Ze =15 mm.

Figure 11 gives the relationship between the crack deviation δ and the trimming width Ze. Obviously, the deviation decreased as the boundary effect became small with the increase of width Ze. And, in order to numerically evaluate the symmetry of the fringe pattern with respect to the laser scanning path, the captured image data was processed to calculate a correlation coefficient for the similarity of fringes on both sides interposing the scanning path. The captured image was divided along the path, then one of them was flipped upside down. An imaginary symmetric fringe pattern was made by combining the original half of image and the flipped one, then it was compared with the captured image to calculate the correlation coefficient between those two images. This was defined as a symmetry factor of fringe pattern and is also shown in Fig. 11. The factor obviously increased as the trimming width, while the deviation decreased.

Finally, the crack deviation behavior is considered in the sight of the distribution of principal stresses difference (σ_1 - σ_2) shown in **Fig. 12**, which was obtained as explained in previous chapter. The figure contains two color contours of principal stresses difference (σ_1 - σ_2) for the trimming width Ze of 15 and 5 mm. Because a half of the principal stresses difference is equal to the maximum shear stress τ_{max}, the high principal stress difference at crack tip causes mode II (in-plane shearing) fracture, which changes the propagation direction [15]. In these figures, the crack and the crack tip in the process are drawn in order to illustrate the relative position of the distribution with respect to the crack. Comparing

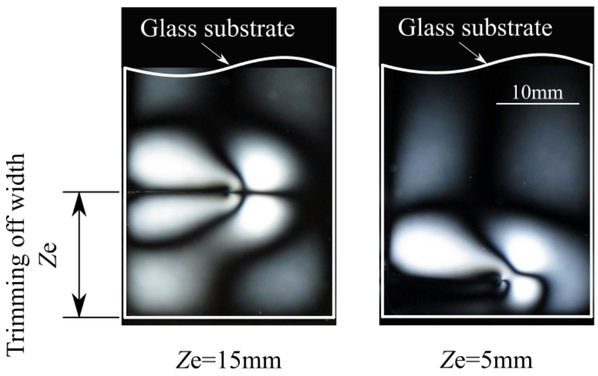

Fig. 10 Isoclinic fringes observed in trimming process.

the distributions for two trimming widths Ze, the maximum value of principal stress difference was almost same. However, the distributions were significantly different. When the shear stress was distributed symmetrically as shown for Ze =15 mm in Fig. 12, the crack propagation path was not bent, while the asymmetrical shear stress distribution caused the deviation of crack for Ze =5 mm.

The results in this section have shown that the deviation of crack propagation can be detected as asymmetry of stress distribution in the trimming process by laser cleaving, too.

5. Conclusions

In this paper, we performed two kinds of laser cleaving tests in which the asymmetric stress distribution was caused.

Through those tests, the photoelastic method was used to observe and to investigate the stress distribution and its effects during the laser cleaving process for the substrates of glass. Obtained results are summarized as follows:

1) Isoclinic and isochromatic fringe patterns were successfully observed by the proposed method during the laser cleaving with a curvilinear path and the trimming process by laser cleaving both.
2) Isoclinic lines were extracted from the fringe patterns, which were observed with the developed experimental set-up for different optic axes of polarizer to identify the direction of principal stresses.
3) The effect of thermally insulated and/or mechanically unconstrained boundary was visualized as the distribution of principal stress direction near the propagating crack in the laser cleaving.
4) The twist of cleaved surface was observed in the laser cleaving with a curvilinear path and the effect of laser scanning speed was examined.
5) Isoclinic fringe patterns made clear that asymmetry of stress distribution caused the crack deviation in the trimming process by laser cleaving.
6) Isochromatic fringe patterns were used with measurement of strain caused within the substrates to provide the contour of principal stress difference near the crack propagating in the trimming process.

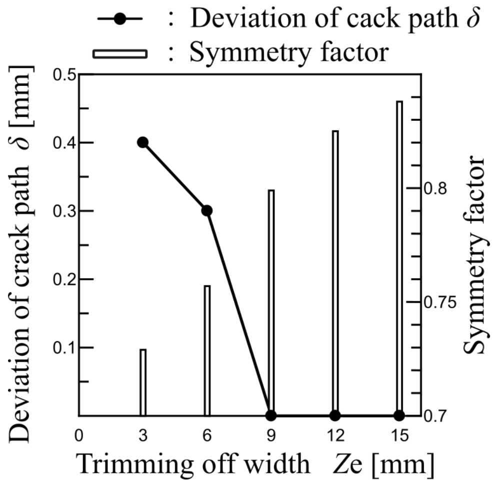

Fig. 11 Deviation of crack δ with trimming off width *Ze*.

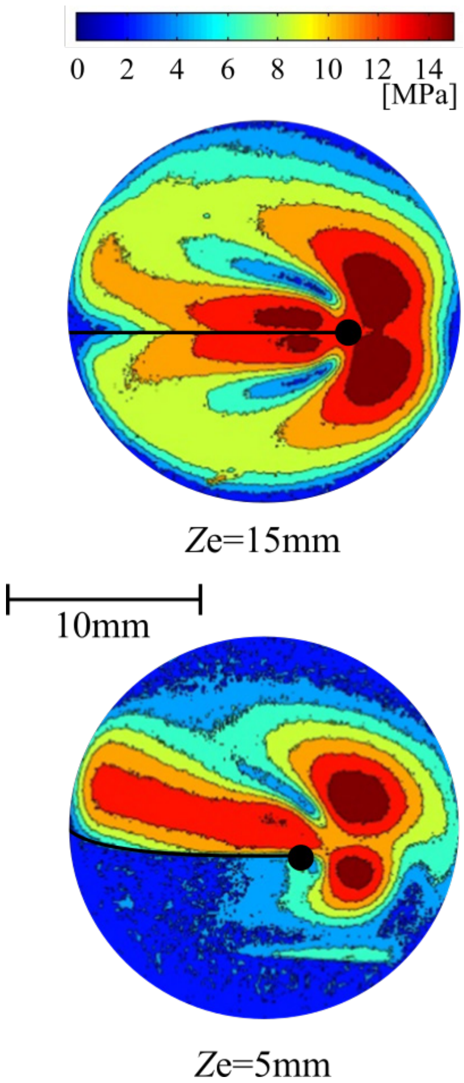

Fig. 12 Distribution of principal stress difference (σ_1 - σ_2).

Acknowledgments

A part of this work was supported by JSPS KAKENHI Grant Number JP17K06081. And authors would like to thank Prof. Dr. Tomoaki Iwai of Kanazawa University, for useful discussions on the photoelastic observation techniques.

References

[1] R. Molian, C. Neuman, P. Shrotriya, P. Malian: J. Manuf. Sci. Eng., 130, (2008) 031008-1.
[2] R. M. Lumley: Am. Ceram. Soc. Bull., 850, (1969) 48.
[3] K. Yamada, K. Oiso, A. Hosokawa, T. Ueda: J. Japan Soc. Precision Eng., 67, (2001) 1861.
[4] K. Yamada, S. Nishioka, A. Hosokawa, T. Ueda: J. Japan Soc. Precision Eng., 69, (2003) 120.
[5] T. Ueda, S. Nishioka, K. Tanaka, K. Yamada, A. Hosokawa: J. Japan Soc. for Abrasive Tech., 53, (2009) 111.
[6] T. Ueda, K. Tanaka, S. Nishioka, K. Yamada, A. Hosokawa: J. Japan Soc. Precision Eng., 75, (2009) 443.
[7] K. Yamada, S. Morita, T. Ueda, A. Hosokawa, R. Tanaka: J. Japan Soc. Precision Eng., 72, (2006) 393.
[8] C. Tsai, C. Liou: J. Manuf. Sci. Eng., 125, (2003) 519.
[9] F. Motomura, Y. Imai, A. Saimoto: J. Solid Mechanics and Mat. Eng., 3, (2009) 529.
[10] C. Tsai, C. Liou: Opt. Lasers Eng., 41, (2004) 189.
[11] K. Yamada, T. Maeda, T. Iwai, K. Sekiya, R. Tanaka: Precision Eng., 47, (2017) 333.
[12] François Cardarelli: "Materials handbook: a concise desktop reference 2nd ed.", (Springer, London, 2008).
[13] J. Dally, W. Riley: "Experimental stress analysis 3rd ed.", (McGraw Hill, New York, 1991) p.431.
[14] D. Hull: Int. J. of Fracture, 70, (1995) 59.
[15] Y. Imai, A. Saimoto, F. Motomura: Trans. of the JSME, 68, (2002) 993.

(Received: May 20, 2019, Accepted: August 25, 2019)